

Optical characterization of $\text{Se}_{90}\text{S}_{10-x}\text{Cd}_x$ thin films.

A.Elfalaky^{a*} K. F. Abdel-El-Rahman^b M.M.Fadel^c

^aDepartment of Physics, Faculty of Science, Zagazig University, Egypt.

^bDepartment of Physics, Faculty of Education, Aain Shams University, Roxy, Cairo, Egypt.

^cHigh Technological Institute, 10th of Ramadan city, Egypt.

Abstract: Thin films of different thicknesses of $\text{Se}_{90}\text{S}_{10-x}\text{Cd}_x$ ($x=0$ and 5) were deposited by thermal evaporation technique onto glass substrates. X-ray diffraction patterns (XRD), differential thermal analysis (DTA) and energy dispersive X-ray spectroscopy (EDX) studies were carried out for samples in powder and thin film forms. XRD indicates that all the deposited thin films have an amorphous structure. The transmittance at normal incidence for these films was measured in the wavelength range 350–2500 nm. Applying Swanepoel's method successfully enabled to determine, with high accuracy, the film thickness, the real index of refraction and imaginary part of index of refraction. Regarding the optical absorption measurements; the type of optical transition and optical band gap were estimated as a function of photon energy. The effect of Cd addition on the refractive index, absorption coefficient and the optical band gap were investigated. The high frequency dielectric constant, the single oscillator energy, the dispersion energy and refractive index dispersion parameter were evaluated. Solar cell criterions have been considered. The results are interpreted in terms of concentration of localized states.

Keywords: Chalcogenides; Amorphous Se-S-Cd; EDX; Optical constants.

I. Introduction:

Amorphous semiconductors are disordered materials. The structure is characterized by the complete absence of long-range order and instead is the existence of short-range order. During the last decades, considerable attention has been focused on amorphous semiconductors specially those known as chalcogenides due to their attractive properties and hence numerous industrial applications. The utilities of such amorphous materials constitute the base of development and applications in solid state technology such as solar cells, solid-state batteries, switching phenomena, xerography, photodiodes, photo-resists in microelectronics, integrated optics, optical imaging, injection laser diodes, optical waveguides, optical data storage and IR detectors [1-6]. Selenium is a major element in the group of chalcogens (S, Se & Te). Amorphous Se (a-Se) has attracted great attention since more than three decades ago [1, 6-8]. This is due to its atomic configuration disorder which is responsible for the existence of localized electronic states within the band gap. Doping of a-Se by different elements modifies its structural network and consequently changes its base properties. It is aimed to investigate the optical properties of a-Se with the addition of both S and Cd. In addition, to reveal the optical constants and other parameters that might help in attainment progressive industrial and technological applications of the compound.

II. Experimental techniques:

Thin films of $\text{Se}_{90}\text{S}_{10-x}\text{Cd}_x$ ($x=0, 5$) were prepared by the conventional melt-quenching technique. The required amounts of the elements of high purity (99.999% pure) were weighted using an electronic balance and sealed in silica ampoules in a vacuum of 10^{-5} Torr. The sealed ampoules were then placed in a constructed oscillatory furnace where the temperature was increased for 3°C per minute up to 950°C and kept at that temperature for 12 h with frequent rocking to ensure the homogenization of the melt. The melt was then rapidly quenched in ice water. Quenched samples were removed from the ampoules by breaking the silica ampoules. The X-ray diffraction patterns of $\text{Se}_{90}\text{S}_{10-x}\text{Cd}_x$ materials were performed by using powder diffractometer (type XPERT-MPDUG, Philips PW 3040) with $\text{CuK}\alpha$ radiation ($\lambda = 1.5406 \text{ \AA}$). The scanning angle was in the range of 4° to 90° .

Thin films of $\text{Se}_{90}\text{S}_{10-x}\text{Cd}_x$ ($x = 0, 5$) of thickness in the range of 121-655 nm were prepared by the vacuum evaporation technique.

A JASCO, V-500, UV/VIS/NIR computerized spectrophotometer is used for measuring optical absorption, reflection and transmission of $\text{Se}_{90}\text{S}_{10-x}\text{Cd}_x$ ($x = 0, 5$) thin films as a function of wave length and incidence photon energy. Applying Swanepoel's method enabled to determine the film thickness, the real (n) and imaginary (k) parts of the complex index of refraction with high accuracy.

III. Results and discussion:

3.1 Structural identification of $Se_{90}S_{10-x}Cd_x$.

X-ray diffraction patterns (XRD), differential thermal analysis (DTA) and energy dispersive X-ray spectroscopy EDX studies were carried out in order to identify the structure and microstructure of $Se_{90}S_{10-x}Cd_x$ ($x=0, 5$) in both powder and thin film forms.

3.1.1 X-ray analysis of $Se_{90}S_{10-x}Cd_x$:

Fig.1 (a & b) shows X-ray diffraction patterns (XRD) for the prepared $Se_{90}S_{10}$ and $Se_{90}S_5Cd_5$ compositions in powder and thin film forms. All the diffraction patterns were examined at room temperature. The diffraction patterns were recorded automatically with a scanning rate of $2\theta = 2$ deg/min and scanning angular range $4^\circ - 90^\circ$. It is observed that the powder form have a polycrystalline nature as a result of existing of different peaks in the patterns. However patterns of thin film show no peaks indicating that the deposited thin films have an amorphous nature.

3.1.2 Differential thermal analysis of $Se_{90}S_{10-x}Cd_x$ ($x=0$ and 5):

Figure 2 shows typical DTA traces of the freshly prepared $Se_{90}S_{10-x}Cd_x$ ($x=0$ and 5), in powder form, at constant heating rate 10 deg. /min. Regarding figure 2, the glass transition temperature T_g , corresponding to the endothermic peak, can be obtained. Values of the glass transition temperature are estimated and given in Table (1). All measurements for the deposited films were carried out at temperatures below T_g to insure that the film samples are in the amorphous state.

3.1.3 Energy Dispersive X-ray analysis of $Se_{90}S_{10-x}Cd_x$ compositions:

The composition constituents in, powder and thin films forms, were investigated using energy dispersive X-ray analysis EDX. Figure 3 (a, b, c and d) show the spectrum of the constituent elements of $Se_{90}S_{10}$ and $Se_{90}S_5Cd_5$ in powder and thin film forms for films of thicknesses 121 nm and 268 nm respectively as a representative examples. Tables (2&3) include the results for powder and thin films of different thicknesses. It can be seen that the obtained constituent elements are nearly stoichiometric for both powder and films forms.

3.2 Optical properties of $Se_{90}S_{10-x}Cd_x$ thin films:

The optical properties are certainly one of the most accurate methods for the determination and investigation of the spectral distributions of optical constants (refractive index n , absorption index k) and hence the absorption coefficient α . Optical constants (n and k) are deduced from the optical transmittance and reflectance data of the deposited films with different compositions and thicknesses in the range ($121 - 655$ nm). An analysis of the absorption coefficient has accomplish, to obtain the optical band gap width and the nature of transitions involved (direct or indirect or both).

3.2.1 Spectral distribution of the transmittance for $Se_{90}S_{10-x}Cd_x$ thin films:

Films of different thicknesses in the range ($121 - 655$ nm) were prepared by thermal evaporation technique as described above in section 2. The optical transmittance and reflectance were measured at room temperature using unpolarized light at normal incidence in the wavelength range ($350 - 2500$ nm). The obtained spectral distribution curves of transmittance are illustrated in figure 4 (a & b) for different thicknesses of $Se_{90}S_{10}$ and $Se_{90}S_5Cd_{15}$ thin films respectively.

3.2.2 Dispersion curves of refractive and absorption indices (n & k).

Several methods were proposed for calculating the optical constants of an absorbing material deposited on non absorbing substrate. These methods could be classified as, polarimetric and spectrophotometric methods (Ellipsometric and interferometric). The spectrophotometric one considers the optical interference occurring between the surfaces of the sample against the incident wavelength. Swanepoel [13] used this optical interference to calculate the optical constants, n and k , of the material and hence find out the optical properties.

According to Swanepoel [13] if the sample thickness, d , is not uniform or slightly tapered, all interference effects will be destroyed and the transmission is smooth curve T_α as shown by the dotted curve in Fig. (5). In case of uniform d , interference effects give rise to a spectrum shown by the full curve in Fig. (5). Such interference fringes can be used to calculate the optical constants of the material as follow:
Considering the thick substrate alone in the absence of a film, the interference-free transmission is given by the well-known expression:

$$T_s = \frac{(1-R)^2}{1-R^2},$$

where

$$R = [(s-1)/(s+1)]^2 \quad \text{or} \quad T_s = \frac{2s}{s^2+1} \quad (1)$$

and

$$s = \frac{1}{T_s} + \left(\frac{1}{T_s^2} - 1 \right)^{\frac{1}{2}} \quad (2)$$

where T_s is the transmission due substrate only and s is the refractive index of the substrate. The basic equation for interference fringes is:

$$2nd = m\lambda \quad (3)$$

where m is either an integer for maxima or half integer for minima respectively. For the case of Fig. 5, the transmission T is a complex function where,

$$T = T(\lambda, s, n, d, \alpha) \quad (4)$$

If s is known, it is convenient to write the above equation in terms of $n(\lambda)$ and the absorbance $x(\lambda)$ as

$$T = T(n, x).$$

Regarding the optical absorption coefficient, α , the spectrum shown in Fig.5 can be divided into three regions, transparent, weak - medium, and strong absorption regions. Following [13] the transmission T in terms of n and s is given through the three regions as:

(i)The transparent region:

In this region $\alpha = 0$ or $x = 1$

$$T_M = \frac{2s}{s^2+1} \quad (5)$$

and

$$T_m = \frac{4n^2s}{n^4 + n^2(s^2+1) + s^2}$$

or

$$n = [M + (M^2 - s^2)^{1/2}]^{1/2} \quad (6)$$

where

$$M = \frac{2s}{T_m} - \frac{s^2+1}{2}$$

T_m is thus function of both n and s , where n can be calculated from T_m using Eq. (6).

(ii) The region of weak and medium absorption

In this region, α is small ($\alpha \neq 0$) and starts to reduce the transmission and $x < 1$. Then

$$n = [N + (N^2 - s^2)^{\frac{1}{2}}]^{\frac{1}{2}} \quad (7)$$

where

$$N = 2s \frac{T_M - T_m}{T_M T_m} + \frac{s+1}{2}$$

Equation (7) can be applied to calculate $n(\lambda)$ from T_M and T_m .

Once $n(\lambda)$ is known; an expression for T_i can be obtained where T_i is found to be as follow:

$$T_i = \frac{2T_M T_m}{T_M + T_m} \quad (8)$$

It can be seen that T_i represents a curve passing through the inflection points of the fringes as shown in Fig. 5.

(iii)The region of strong absorption:

In the region of strong absorption, the interference fringes disappear. Values of n can be estimated by extrapolating the values calculated in the other regions of the spectrum. For very large α four curves T_M , T_o , T_i and T_m converge to a single curve T_o .

$$x \approx \frac{(n+1)^3(n+s^2)}{16n^2s} T_o \quad (9)$$

The thickness of the film could be determined by assuming that n_1 and n_2 are the refractive indexes at two adjacent maxima (or minima) at wavelengths λ_1 and λ_2 . Applying Eq. (3), then

$$d = \lambda_1 \lambda_2 / [2 (\lambda_1 n_2 - \lambda_2 n_1)] \quad (10)$$

For the studied $Se_{90}S_{10-x}Cd_x$ ($x = 0$ and 5) films, the optical spectrum in the wavelength range (350-2500 nm) are shown in Fig. (4). The spectral envelopes of the transmission $T_{max}(\lambda)$ and $T_{min}(\lambda)$ are computed using a graphical method.

The optical constants, n , and k , of $Se_{90}S_{10-x}Cd_x$ ($x=0$ and 5) films were calculated, by developing a computer program, using Swanepoel's equations. Figures (6&7) show the spectral distribution of both n and k respectively. It is clearly evident from figures (6&7), in consistence with previously reported results [12], that the values of n and k for $Se_{90}S_5Cd_5$ films are smaller than those for $Se_{90}S_{10}$ films all over the whole range of the studied wavelength. Such trend can be attributed to the chemical bond Se-Cd which is stronger than Se-S one. Moreover the addition of Cd to Se-S amorphous system tends to increase the saturated bonds and hence reduces the number of excited electrons from the filled states to the empty states.

3.2.3 Analysis of refractive index n data.

The high frequency dielectric constant can be obtained from analyzing the refractive index n data via two approaches [14]. The first one regards the vibrational modes of dispersion of the free carries and the lattice. On the other hand, the second one considers the dispersion arising from the bound carriers in an empty lattice.

a) First approach:

In the near infrared spectral region, where the frequency is relatively high, the real part ϵ_1 of the complex dielectric constant can be written as $\epsilon_1 = n^2$ then [15]:

$$n^2 = \epsilon_1 = \epsilon_\infty - \frac{e^2}{4\pi^2 c^2 \epsilon_0} \frac{N}{m^*} \lambda^2 \quad (11)$$

where, ϵ_∞ is the high frequency dielectric constant, e is the electronic charge, c is the velocity of light, ϵ_0 is the free space dielectric constant and N/m^* is the ratio of free carrier concentration (N) to the free carrier effective mass (m^*). The plot of n^2 versus λ^2 is shown in Fig. (8) for $Se_{90}S_{10-x}Cd_x$, ($x=0$ and 5) films. Extrapolating the

linear part of the plot in the region of high wavelength to zero wavelength gives the value of ϵ_∞ and from the slope of this line, the value of (N/m^*) for the investigated material film can be calculated according to equation 20. The obtained values of ϵ_∞ (1) and N/m^* are given in Table (4) for studied compositions.

b) Second approaches:

At high frequency the properties of the composition under investigation could be treated as that of a single oscillator at wavelength λ_o for every composition. The high frequency dielectric constant can be calculated using the following [16]. If n_o is the refractive index of an empty lattice at infinite wavelength, the index will vary as:

$$(n_o^2 - 1) / (n^2 - 1) = 1 - (\lambda_o / \lambda)^2 \quad (12)$$

where λ_o and n_o are evaluated from plots of $(n^2 - 1)^{-1}$ against λ^{-2} shown in figure (9) for both film compositions, the values of ϵ_∞ (2) and λ_o are given in Table (4). Values of ϵ_∞ obtained by both methods are in good agreement with each other. The reason for this agreement, despite the difference in procedures used, is that the lattice vibrational and plasma frequencies are well separated from the absorption band-edge frequency.

Equation (21) can be also expressed as [17]

$$(n^2 - 1) = (S_o \lambda_o^2) / [1 - (\lambda_o / \lambda)^2] \quad (13)$$

$$[n^2 - 1] = E_d E_s / [E_s^2 - (hv)^2] \quad (14)$$

where hv is the photon energy, E_s is the single oscillator energy and E_d is the dispersion energy.

Values of the parameters E_s and E_d were evaluated by plotting $(n^2 - 1)^{-1}$ versus $(hv)^2$ and fitting it to a straight line as shown in Fig. (10) for deposited $Se_{90}S_{10}$ and $Se_{90}S_5Cd_5$ thin films. The obtained values of the single oscillator parameters E_s , E_d , S_o , E_s and E_s/S_o for the studied films are given also in Table (4). It is to be noted that the refractive index dispersion parameter is given by the ratio E_s/S_o .

3.2.4 Analysis of the absorption index k data:

The spectral distribution of the absorption coefficient α of a semiconductor near the fundamental edge is of great importance for the investigation of the allowed transitions, as well as, the energy band structure. At different values of the wavelength (λ) in the considered spectrum and using the corresponding values of (k) , the absorption coefficient (α) of $Se_{90}S_{10}$ and $Se_{90}S_5Cd_5$ films are calculated using the equation $\alpha = 4 \pi k / \lambda$. The obtained values of α as a function of photon energy (hv) are illustrated in Fig. (11). It can be easily seen that α has very high value in order of $10^5 cm^{-1}$. Regarding the highest intensity and flux density of the solar spectrum, as shadowed area in inset of Fig.(11), it can be noticed that the region of highest absorption of the studied compounds matches well with such spectrum.

The variation of the absorption coefficient with photons energy obeys the relation [21]:

$$\alpha(v) = [A (hv - E_g^{opt})^r] / hv \quad (15)$$

where A is the edge width parameter representing the film quality, which is calculated from the linear part of this relation, E_g^{opt} is the optical energy gap of the material and r determines the type of transition, The parameter r has the value $1/2$ for the direct allowed transitions and 2 for the indirect allowed transitions. The usual method for the determination of the value of E_g^{opt} involves plotting a graph of $(\alpha hv)^{1/r}$ against hv . Figs. (12 & 13) show plots of $(\alpha hv)^{1/2} = f(hv)$ and $(\alpha hv)^2 = f(\lambda)$ respectively. It is clear that $(\alpha hv)^{1/2} = f(hv)$ is linear function. This linearity indicates the existence of the indirect allowed transitions.

The values of the energy gap E_g^{opt} is determined from the intercept of the extrapolation to zero absorption with the photon energy axis. Values of the optical band gap E_g^{opt} and A are given also in Table (5).

Optical energy gap for amorphous semiconductors can be determined also from the following equation [22].

$$h^2 v^2 \epsilon_2 \sim (hv - E_g^{opt})^2 \quad (16)$$

where $\epsilon_2 = 2nk$ (ϵ_2 is the imaginary part of the dielectric constant). The absorption in this region is most easily explained by indirect transitions between the so-called extended states in both valance and conduction bands [22]. Fig. (14) shows a plot of $hv(\epsilon_2)^{1/2}$ against hv , which gives a linear part satisfying equation (16) for indirect

optical transitions. The extrapolation of this linear part yields E_g^{opt} . The obtained values of optical energy gap are given in Table (5) and they are in good agreement with those obtained from $(\alpha hv)^{1/2}$ versus hv relation Fig. (12) for both compositions. According to the values of E_g^{opt} and A it can be said that S replacement by Cd tends to increase the energy gap and decrease the edge width parameter A. The increase of energy gap with the addition of Cd can be ascribed to the decrease of the density of the localized states associated with the saturated Se-Cd bonds. Considering such values of energy gap, the absorption coefficient and the solar spectrum distribution, the studied chalcogenides are well coupled with the solar spectrum. In accord such materials are considered as promising material for solar cell and photovoltaic applications.

IV. Conclusions:

Based on transmission spectrum data only the spectrum of optical constants, n and k were determined with good accuracy for amorphous thin films of $Se_{90}S_{10}$ and $Se_{90}S_5Cd_5$ chalcogenides utilizing Swanepoel methodology. n, k and α have been found to decrease with the increase of Cd on the expense of S. In accord Se-Cd is optically less dense than Se-S. On the other hand despite the values of the parameters ϵ_g , λ_o , S_o and A decrease with the addition of Cd instead of S, while the values of E_s , E_d , N/m^* and E_g^{opt} seem likely to increase with Cd substitution. The optical transition has been concluded to be indirect optical transitions. The replacement of S by Cd achieves remarkable changes in the optical constants. Such changes can be attributed to difference between the Se-S and Se-Cd bonds. The former is unsaturated bond while the latter is saturated one. The reduction in the number of unsaturated bonds, due to Cd addition on the expense of S, conceals the density of defects. Hence the density of localized states in the band structure and accordingly band gap increases and absorption coefficient decreases. Regarding the distribution of solar spectrum, the absorption coefficient and the energy gap of $Se_{90}S_{10}$ and $Se_{90}S_5Cd_5$ chalcogenides such materials are expected to be promising materials for photovoltaic and solar cells applications

References

- [1]. N. F. Mott and E. A. Davis, "Electronic Processes in Non-Crystalline Materials", (Clarendon press, Oxford) 1971; *ibid.* 1979.
- [2]. P. G. Le Comber and J. Mort, "Electronic and Structural Properties of Amorphous Semiconductors" (Academic press London and NewYork) 1973.
- [3]. D. Adler, "Physical Properties of Amorphous Materials", Ed. D. Adler, B. B. Schwartz and M. C. Steele, (Plenum Press) 1985.
- [4]. E. Owen, " Electronic and Structural Properties of amorphous Semiconductors" , Proc. Of 13th Session of the Scottish Universities, 161 (1972).
- [5]. R. Elliott, "Physics of Amorphous Materials", John Wiley & Sons, (Inc., New York) 1990.
- [6]. F. Kotkata, D.Sc. Thesis, Hungarian Academy of Sciences, Budapest, 1993.
- [7]. F. Kotkata, J. Mater. Sci., 27(1992) 4847; *ibid.* 27 (1992) 4858.
- [8]. G. Gordillo and E. Romero, Thin Solid Films, 484 (2005) 352.
- [9]. S.Al-Hazmi, Physica B 404 (2009) 1354–1358.
- [10]. Shamshad A. Khan and A. A. Al-Ghamdi, Materials Letters 63 (2009) 1740–1742.
- [11]. Shamshad A. Khan, F.S. Al-Hazmi, S. Al-Heniti, A.S. Faidah and A.A. Al-Ghamdi, current applied physics 10 (2010) 145-152.
- [12]. Shamshad A.Khan, J.K.Lal and A.A.Al-Ghamdi, Optics & Laser Technology 42 (2010) 839–844.
- [13]. R. Swanepoel, J. Phys. E: Sci. Instrum., 16 (1983) 1215.
- [14]. J.N, Zemel, J.D. Jensen, R.B. Schoolar, Phys. Rev. A, 140 (1965) 330.
- [15]. T. S. Moss, G. J. Burrell, E. Ellis, "Semiconductor Opt-Electronics", (Butterworths, London) 1973.
- [16]. A. E. Bekheet, Eur. Phys. J. Applied Physics, 16 (2001) 187.
- [17]. P. A. Lee, G. Said, R. Davis and T. H. Lim, J. Phys. Chem. Solids 30(1969)2719.
- [18]. S. H. Wemple and M. DiDomenico, Phys. Rev. B3., (1971) 1338.
- [19]. S. H. Wemple and M. DiDomenico, Phys. Rev. B7., (1973) 3767.
- [20]. D. Armitag, D.E. Brodi, and P. C. Eastman, Con. J. of phys. 49 (1971) 1662.
- [21]. E. A. Davis and Mott, Phil. Mag., 22 (1970) 903.
- [22]. J. Tauc, R. Grigorovici and A. Vancu, Phys. Stat. Solid 15 (1966) 627.

Figure captions

Fig. 1: X-ray diffraction patterns of $Se_{90}S_{10-x}Cd_x$ for :

- a) $x = 0$ b) $x = 5$

Fig.2 : Differential thermal analysis DTA of $Se_{90}S_{10-x}Cd_x$ for :

- a) $x = 0$ b) $x = 5$

Fig.(3): EDX for $Se_{90}S_{10-x}Cd_x$:

- a) $x=0$ in powder form. b) $x=0$ film of thickness 121 nm.
c) $x=5$ in powder form. d) $x=5$ film of thickness 268 nm.

Fig.(4): Spectral distribution of transmittance for deposited thin films of $Se_{90}S_{10-x}Cd_x$ for : a) $x = 0$ b) $x = 5$

Fig.(5): Simulated transmission spectrum (full curve) and finite glass substrate with transmission Ts. Curves TM, Ta, Ti and Tm are those according to the text.

Fig.(6): Dependence of the refractive index n on the wavelength λ for the deposited $Se_{90}S_{10}$ and $Se_{90}S_5Cd_5$ thin films.

Fig.(7): Dependence of the absorption index k on the wavelength λ of the deposited $Se_{90}S_{10}$ and $Se_{90}S_5Cd_5$ thin films.

Fig.(8): Plots of n^2 against λ^2 for the deposited $Se_{90}S_{10}$ and $Se_{90}S_5Cd_5$ thin films.

Fig.(9): Plots of $(n^2 - 1)^{-1}$ against λ^{-2} for the deposited $Se_{90}S_{10}$ and $Se_{90}S_5Cd_5$ thin films.

Fig.(10): Plots of $(n^2 - 1)^{-1}$ against $(hv)^2$ for the deposited $Se_{90}S_{10}$ and $Se_{90}S_5Cd_5$ thin films.

Fig.(11): Dependence of the absorption coefficient α on the photon energy (hv) for the deposited $Se_{90}S_{10}$ and $Se_{90}S_5Cd_5$ thin films. α against λ as inset.

Fig.(12): dependence of $(\alpha hv)^{1/2}$ on the photon energy (hv) for the deposited $Se_{90}S_{10}$ and $Se_{90}S_5Cd_5$ thin films.

Fig.(13): dependence of $(\alpha hv)^2$ on the photon energy (hv) for the deposited $Se_{90}S_{10}$ and $Se_{90}S_5Cd_5$ thin films.

Fig.(14): Dependence of $hv(\epsilon_2)^{1/2}$ on the photon energy (hv) for the deposited $Se_{90}S_{10}$ and $Se_{90}S_5Cd_5$ thin films.

Figures

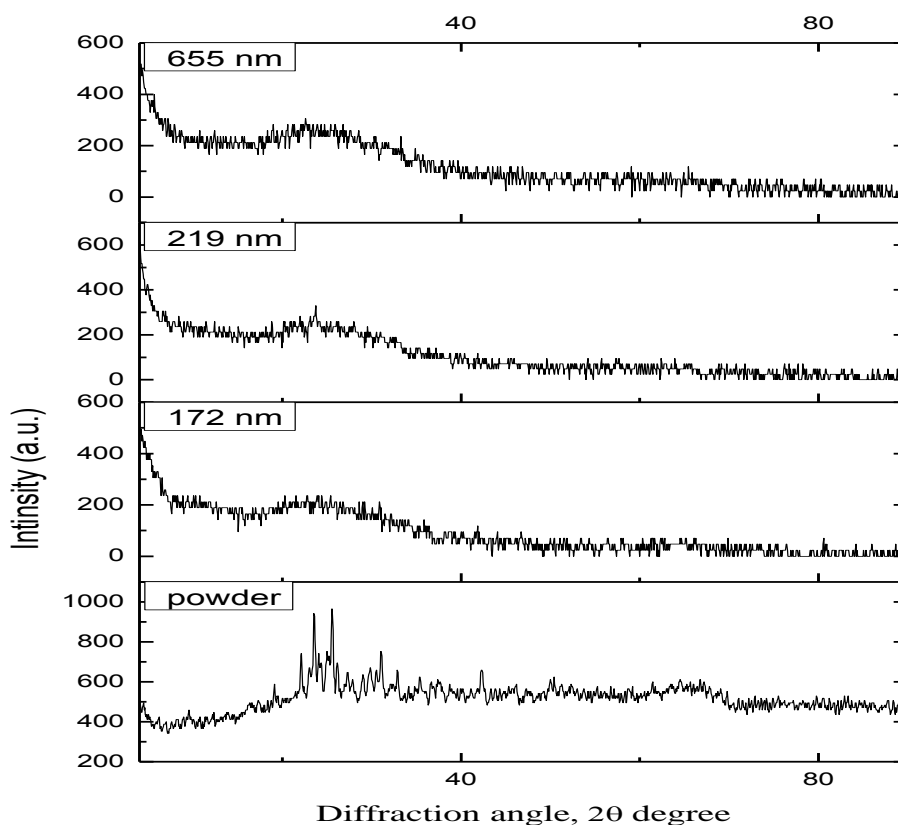


Fig. 1 (a)

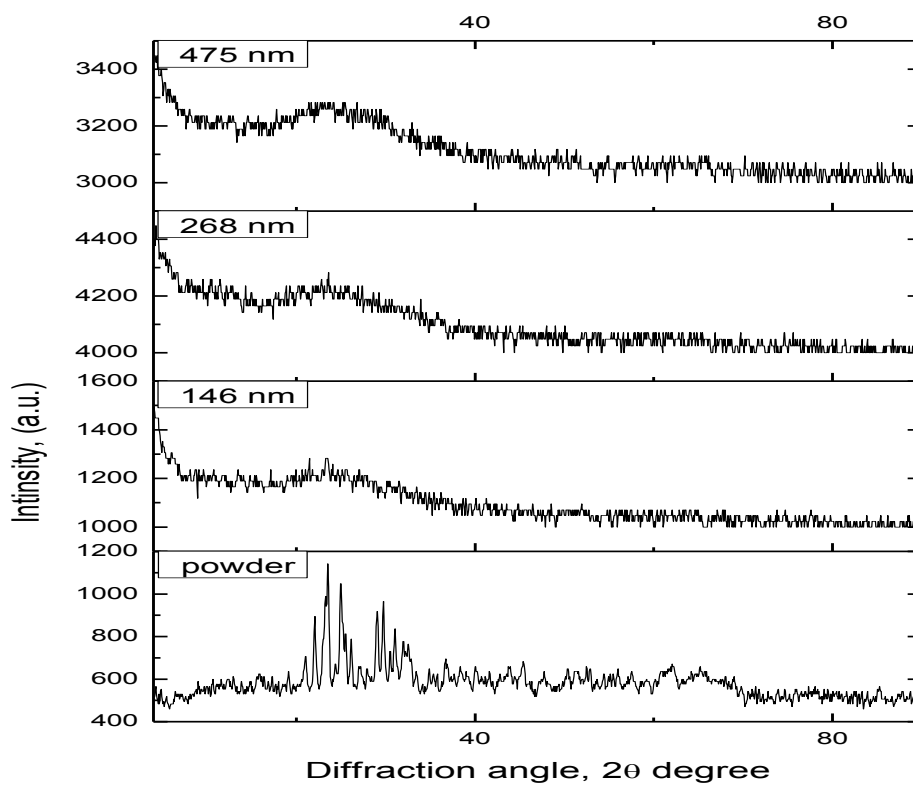


Fig. 1 (b)

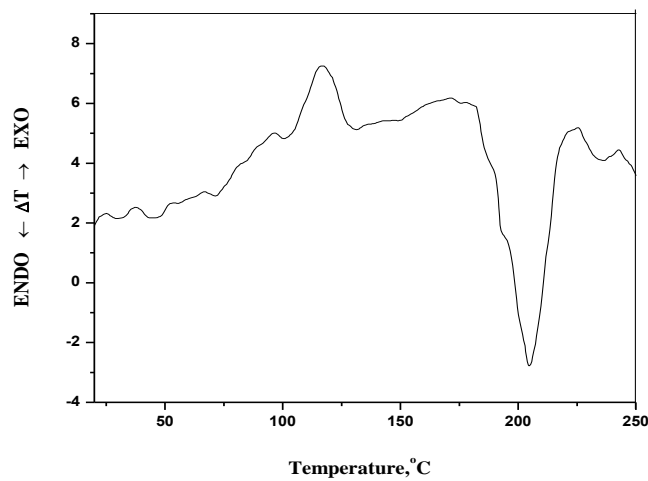


Fig. 2(a)

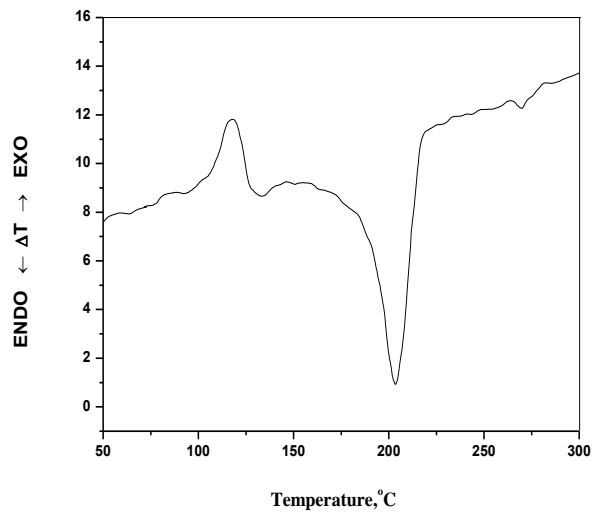


Fig. 2 (b)

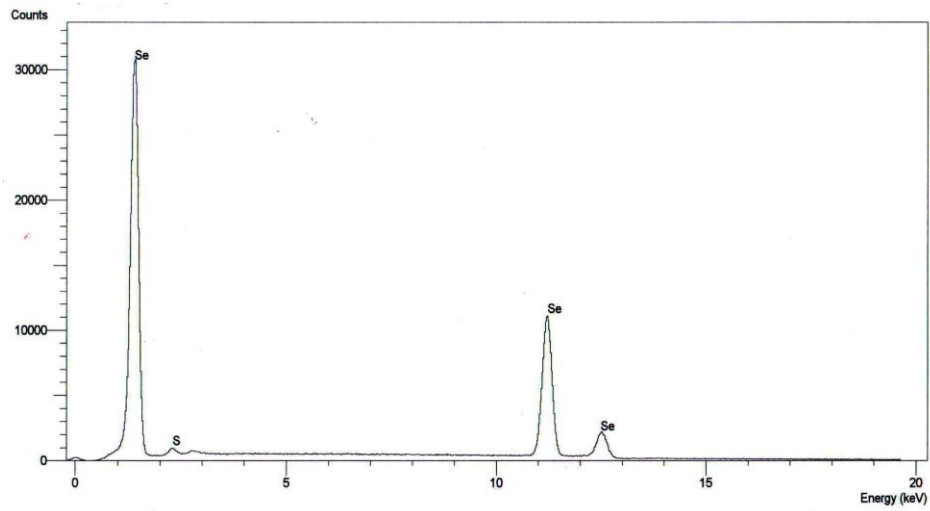


Fig. 3 (a)

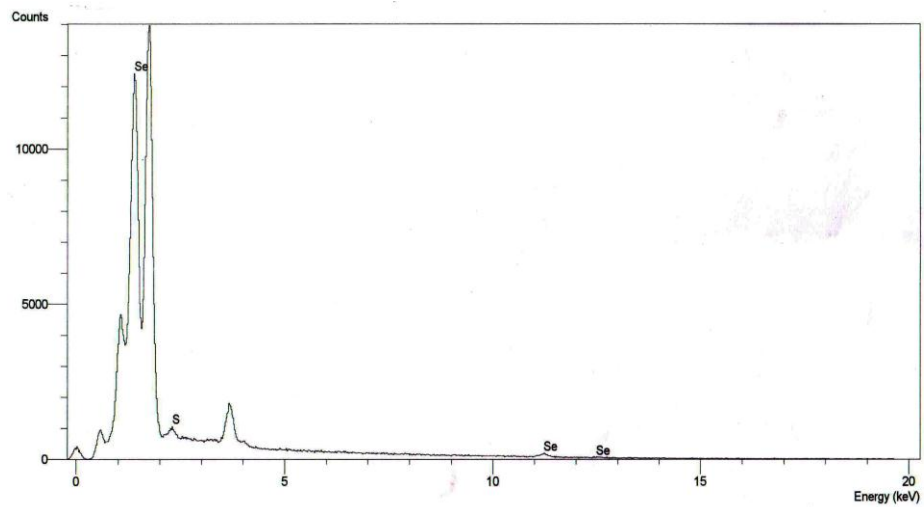


Fig. 3 (b)

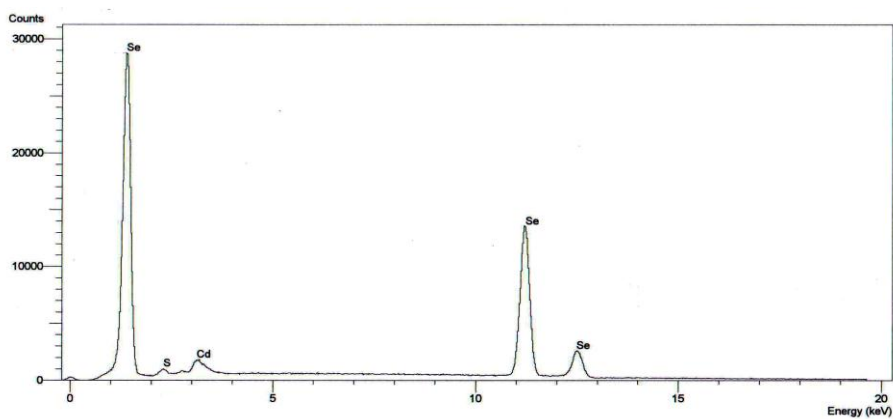


Fig. 3 (c)

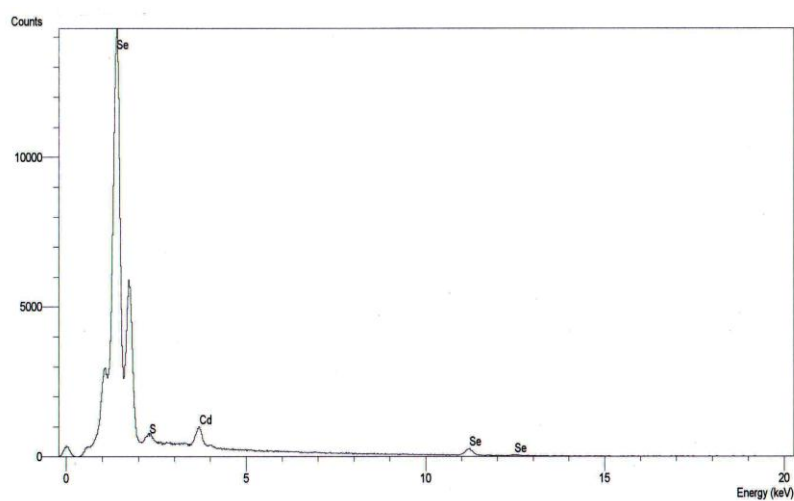


Fig. 3 (d)

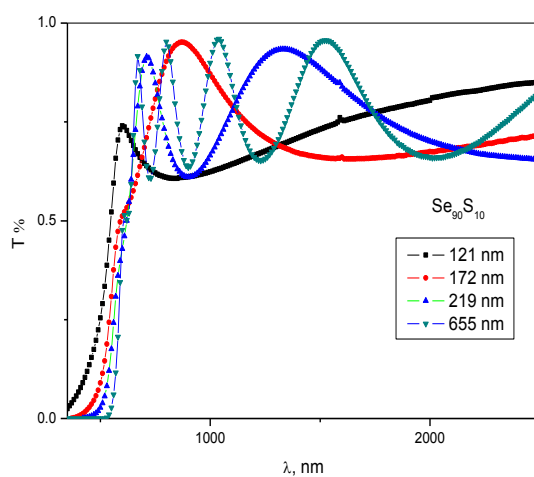


Fig. 4 (a)

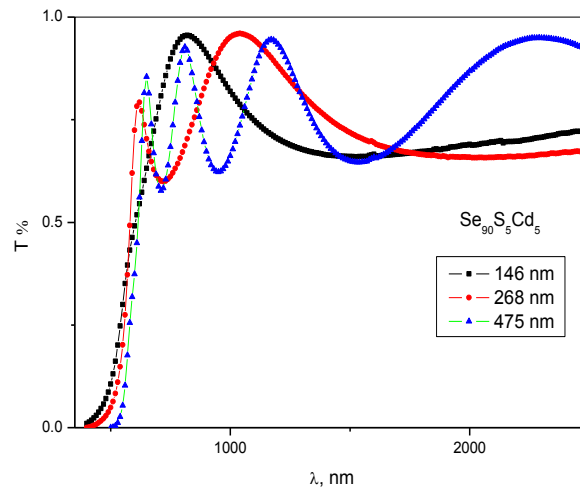


Fig. 4 (b)

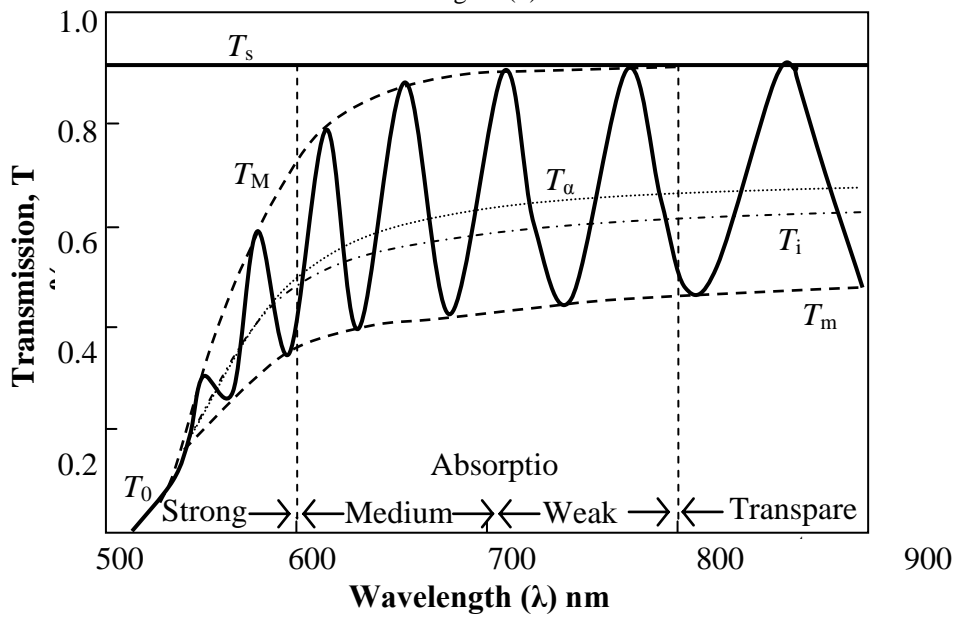


Fig. (5)

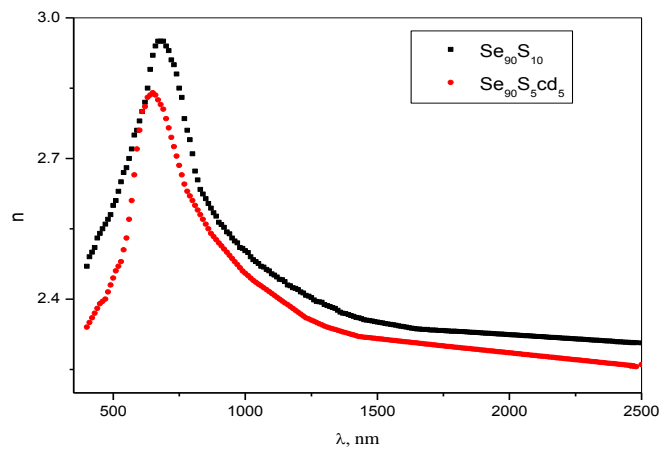


Fig.(6)

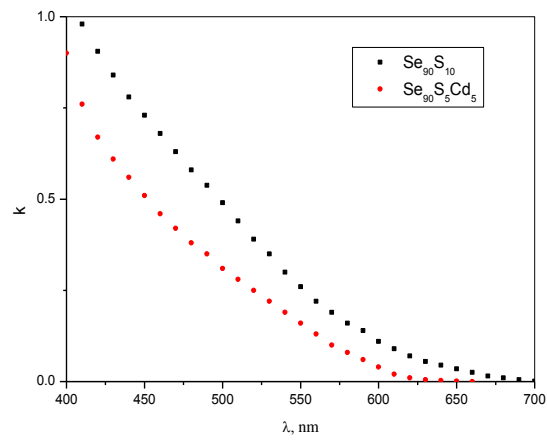


Fig.(7)

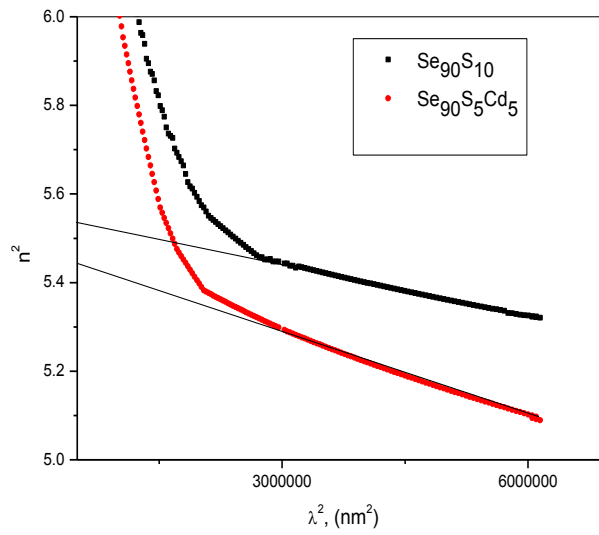


Fig. (8)

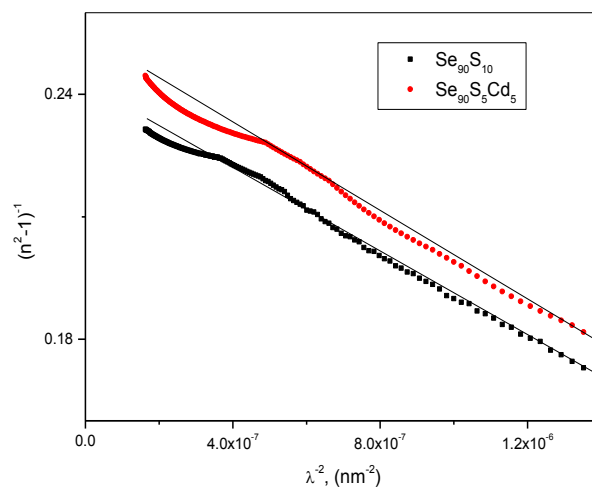


Fig. (9)

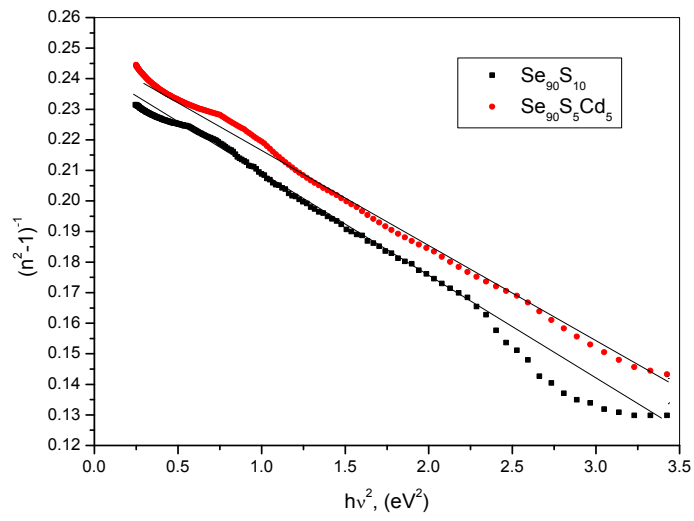


Fig. (10)

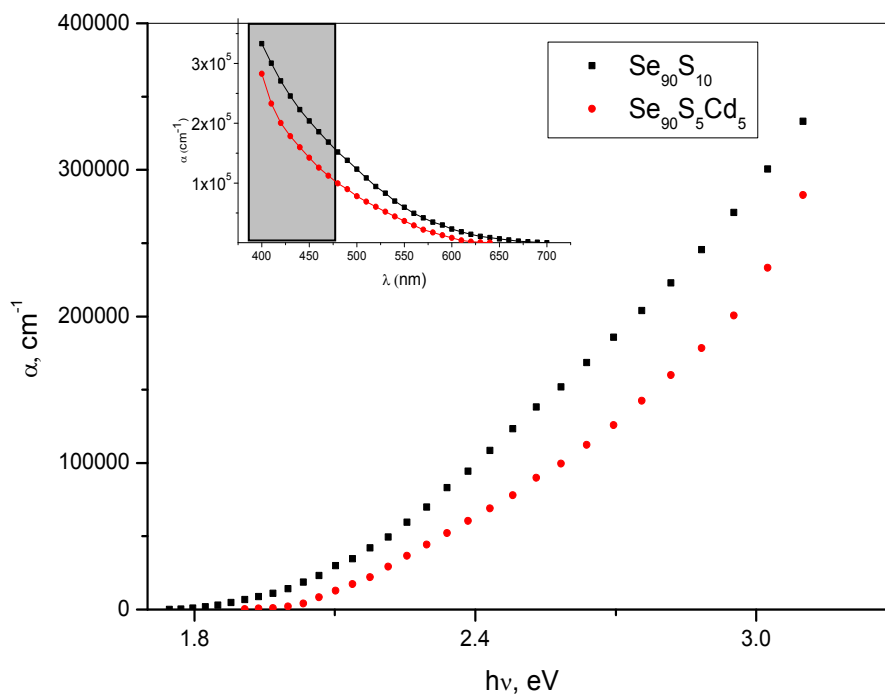


Fig. (11)

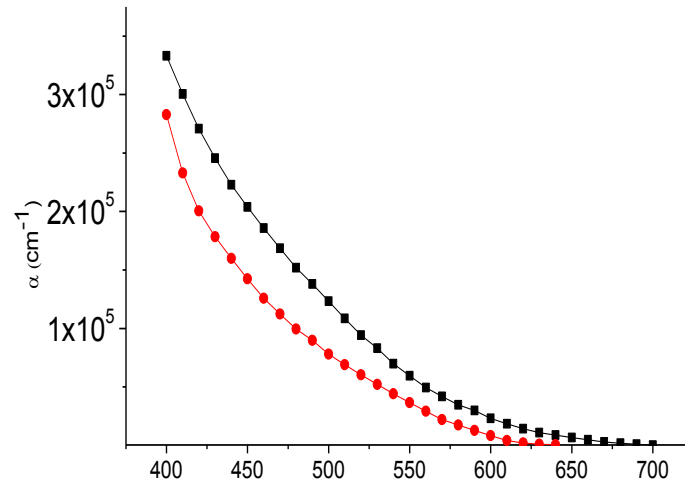


Fig. (12)

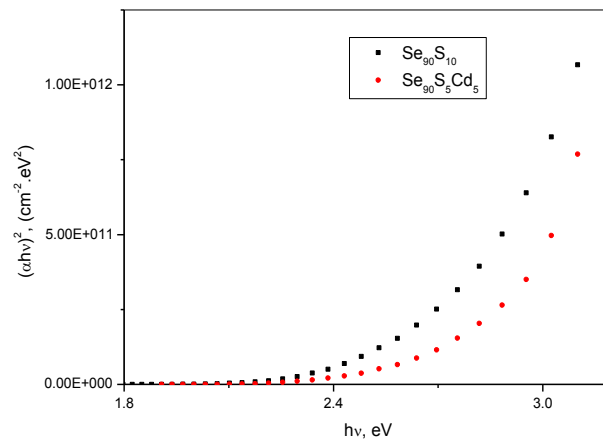


Fig. (13)

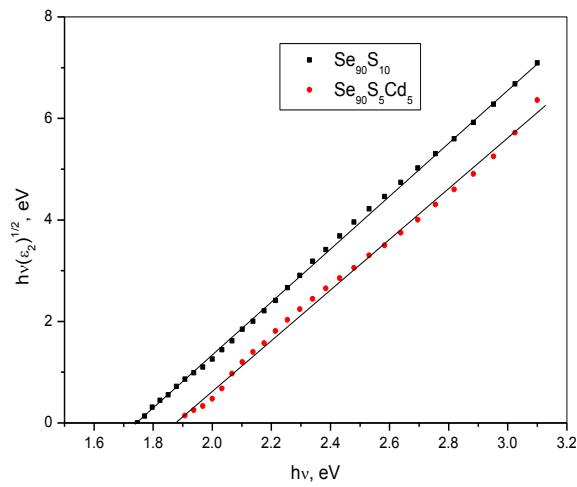


Fig.(14)

Tables

Table (1): Values of T_g for $Se_{90}S_{10-x}Cd_x$ ($x=0$ and 5) films

Table (2): Elemental analysis of $Se_{90}S_{10}$

Table (3): Elemental analysis of $Se_{90}S_5Cd_5$

Table (4): Parameters derived from refractive index n for deposited $Se_{90}S_{10}$ and $Se_{90}S_5Cd_5$ films.

Table (5): Parameters derived from absorption coefficient index k for deposited $Se_{90}S_{10}$ and $Se_{90}S_5Cd_5$ films

Tables

Table (1):

Composition	T_g , K
$Se_{90}S_{10}$	205.28
$Se_{90}S_5Cd_5$	204.17

Table (2):

At %	Se	S	Cd	Formula
Bulk	91.02	8.98	$Se_{90}S_{10}$	$Se_{91.02}S_{8.98}$
Film, d=121 nm	90.07	9.93	$Se_{90}S_{10}$	$Se_{90.07}S_{9.93}$
Film, d=172 nm	89.795	10.205	$Se_{90}S_{10}$	$Se_{89.795}S_{10.205}$
Film, d=218 nm	90.98	9.02	$Se_{90}S_{10}$	$Se_{90.98}S_{9.02}$
Film, d=655 nm	91.55	8.45	$Se_{90}S_{10}$	$Se_{91.55}S_{8.45}$

Table (3):

At %	Se	S	Cd	Formula	Se
Bulk	89.81	4.15	6.04	$Se_{90}S_5Cd_5$	$Se_{89.81}S_{4.15}Cd_{6.04}$
Film, d=146 nm	91.47	3.911	4.619	$Se_{90}S_5Cd_5$	$Se_{91.47}S_{3.911}Cd_{4.619}$
Film, d=268 nm	91.31	4.81	3.88	$Se_{90}S_5Cd_5$	$Se_{91.31}S_{4.81}Cd_{3.88}$
Film, d=475 nm	89.05	5.275	5.675	$Se_{90}S_5Cd_5$	$Se_{89.05}S_{5.275}Cd_{5.675}$

Table (4):

Parameter	deposited $Se_{90}S_{10}$	deposited $Se_{90}S_5Cd_5$
$\epsilon(1)$	5.56	5.46
$\epsilon(2)$	5.13	4.99
λ , nm	460.3	451.7
S , m^{-2}	1.9486×10^{13}	1.95309×10^{13}
E_s , eV	2.6556	2.756
E_s/S , eV/m^2	1.3628×10^{-13}	1.41123×10^{-13}
E_d , eV	10.978	10.994
$N/m^2 \cdot m^{-3} \cdot kg^{-1}$	4.92×10^{46}	7.277×10^{46}

Table (5):

Parameter	deposited $Se_{90}S_{10}$ thin films	deposited $Se_{90}S_5Cd_5$ thin films
E_g^{opt} , eV From equation (24)	1.762	1.887
E_g^{opt} , eV From equation (25)	1.747	1.873
A , $cm^{-1}eV^{-1}$	570025	544555

